Direct Relationship between Magnetism and MnO$_6$ Distortions in La$_{1-x}$Ca$_x$MnO$_3$

C. H. Booth,[1,2,*] F. Bridges,[2] G. H. Kwei,[3] J. M. Lawrence,[1] A. L. Cornelius,[3] and J. J. Neumeier[3,†]

[1]*Department of Physics and Astronomy, University of California, Irvine, California 92697*
[2]*Physics Department, University of California, Santa Cruz, California 95064*
[3]*Los Alamos National Laboratory, Los Alamos, New Mexico 87545*

Measured distortions of the Mn-O bond length distribution from x-ray-absorption fine-structure measurements are found to relate linearly to the doped hole concentration x at room temperature in La$_{1-x}$Ca$_x$MnO$_3$. Comparison of the distortions above and below T_c for colossal magnetoresistor (CMR) samples gives an estimate of the number of delocalized holes n_{dh}, and we find that $\ln(n_{dh}) \propto M$ (magnetization). These results are complementary to resistance measurements that show that $\ln(\rho) \propto -M$. We have thus established the functional relationship between the electronic, spin, and lattice degrees of freedom in the CMR perovskites. [S0031-9007(97)05093-X]

The La$_{1-x}$A$_x$MnO$_3$ series (where A is a divalent metal such as Ca, Sr, Ba, or Pb) demonstrates many interesting electronic, magnetic, and structural properties. In particular, samples with $A =$ Ca and $0.2 \lesssim x \lesssim 0.48$ [1] have coincident metal-insulator and paramagnetic (PM) to ferromagnetic (FM) transitions. Samples with other values of x are insulators regardless of the magnetic state. A large peak in the magnetoresistance (MR) was first measured in La$_{0.8}$Sr$_{0.2}$MnO$_3$ near room temperature by Volger [2]. The basic mechanism of electronic transport has long been thought to be the double exchange (DE) mechanism [3]. Recent re-examinations of the MR in these materials have dubbed the effect as "colossal" magnetoresistance [4], or CMR, because of the enhancements of the effect that can be obtained by using thin films or varying the stoichiometry [5]. The understanding of the transport in these materials was advanced when Millis *et al.* pointed out that the MR expected from the DE model is much smaller than is actually measured [6]. This discrepancy can be explained by including a large lattice distortion above T_c, which is at least partially removed below T_c [7]. Indeed, there is a growing body of literature supporting this view. Evidence supporting polaronic transport above T_c includes resistivity [8] and thermoelectric power [9] measurements. A large isotope shift of T_c (~ 20 K) with O^{18} substitution [10] indicates a strong spin-lattice coupling. Perhaps the most convincing studies showing a connection between the electronic properties and the lattice are the local-structure measurements of the Mn-O bond length distribution [11–14]. These studies show that the Mn-O environment is distorted above T_c by an amount roughly consistent with the Jahn-Teller (JT) distortion of the MnO$_6$ octahedra in LaMnO$_3$, and that this distortion is at least partially removed in the FM state.

Obtaining quantitative relations between the electrical, magnetic, and structural properties is an important step towards understanding the physics of the CMR materials. For instance, Hundley *et al.* [8] have shown that the resistance and the magnetism relate simply by $\ln(\rho) \propto -M$.

A relation involving the lattice has not previously been reported. Since the magnetization is directly coupled to the conduction and the magnitude of the JT distortions, the size of the distortions should be an intrinsic function of the magnetization. Likewise, since these hopping charges are the charge carriers, the distortions, magnetization and resistivity should all be directly related. As shown in Ref. [13], the temperature dependence of the disorder of the MnO$_6$ octahedra in the metallic state is probably a function of the magnetism, rather than normal thermal (Debye) behavior.

In this Letter, we present x-ray-absorption fine-structure (XAFS) data that directly relate the structural distortions to the magnetization of the CMR perovskites. A simple model is presented relating the magnitude of the distortions to the localized hole concentration above T_c. By extending these results below T_c, we can measure the number of holes that become delocalized charge carriers. This *structural* measurement of the delocalized hole concentration is found to relate exponentially to the magnetization, in agreement with the transport measurements which find a related dependence of the resistivity.

Powder samples of La$_{1-x}$Ca$_x$MnO$_3$ were prepared by solid state reaction of La$_2$O$_3$, CaCO$_3$, and MnO$_2$ with repeated grindings and firings at temperatures up to 1400 °C, with a final slow cool at 1 °C per min. The dc magnetization was measured using a commercial SQUID magnetometer. Figure 1(a) shows the magnetization for the CMR samples. T_c's for $x = 0.21$, 0.25, 0.30 are estimated to be 208 ± 5, 240 ± 5, and 260 ± 5 K, respectively, by extrapolation of M at maximum slope.

All XAFS data were collected at the Stanford Synchrotron Radiation Laboratory (SSRL). Mn K edge data were collected in transmission mode on beam line 2-3 using Si(220) double monochromator crystals. The powders were reground, passed through a 400-mesh sieve, and brushed onto scotch tape. Layers of tape were stacked to obtain absorption lengths such that $\mu_{Mn}t \sim 1$ for each sample. Generally, three scans were collected at each
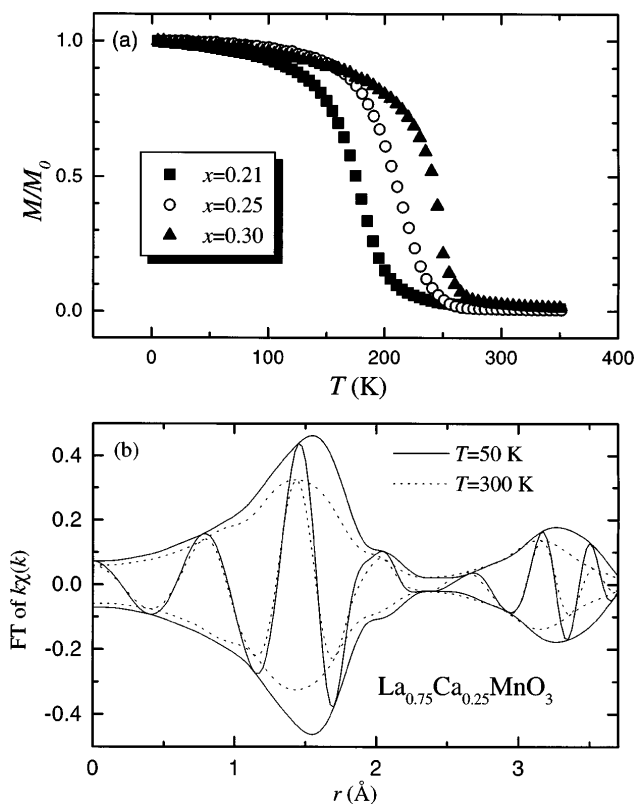
FIG. 1. (a) Magnetization (normalized to M at $T = 5$ K) vs T for $La_{1-x}Ca_xMnO_3$ with $x = 0.21$, 0.25, and 0.30. The fields used were 5000, 1500, and 5000 Oe, respectively. (b) Fourier transform (FT) of $k\chi(k)$ vs r for the $x = 0.25$ sample at $T = 50$ K (solid) and 300 K (dotted). The outer envelope is the amplitude and the oscillating line is the real part of the complex transform. The first peak in the amplitude at ~1.5 Å contains components of several Mn-O distances.

by the absorbing and neighboring atoms. The first peak in the amplitude at ~1.5 Å in Fig. 1(b) contains contributions from several Mn-O bond lengths. For instance, in $LaMnO_3$, the Mn-O pairs in the MnO_6 octahedra include two at ~1.91 Å, two at ~1.97 Å, and two at ~2.15 Å [17]. This distortion is due to the Jahn-Teller effect. In $CaMnO_3$, the Mn^{4+} ions are not Jahn-Teller active, and therefore all six Mn-O bonds are ~1.89 Å long [18]. The peaks at larger r contain information about more distant neighbors to the Mn and will be discussed elsewhere [19].

As the temperature is lowered below T_c, the amplitude of the Mn-O peak grows by ~40% [Fig. 1(b)], corresponding to a narrower Mn-O bond length distribution. Most of this growth cannot be explained by thermal, Debye narrowing of this distribution [13]. Figure 2 shows fit results for the Mn-O distribution width σ as a function of temperature. Since XAFS cannot resolve even the well-defined distortion in $LaMnO_3$, we chose to fit the Mn-O distribution to a single Gaussian distribution, and describe distortions and disorder only in terms of σ. The temperature dependence of σ for $CaMnO_3$ follows a correlated-Debye model, with practically no static distortion. The temperature dependence of $LaMnO_3$ is not clear from these data, although ~0.08 Å of additional static distortion due to the JT distortions is required to fit the data. The CMR samples have a similar temperature dependence as $CaMnO_3$ above T_c (PM insulating state), and have ~0.06 Å of static disorder. As the temperature is lowered through T_c, the Mn-O bond length distribution narrows, becoming nearly as narrow as in $CaMnO_3$, especially for $x = 0.30$. The log of the polaron contribution to the width can be shown to be linear in M, which
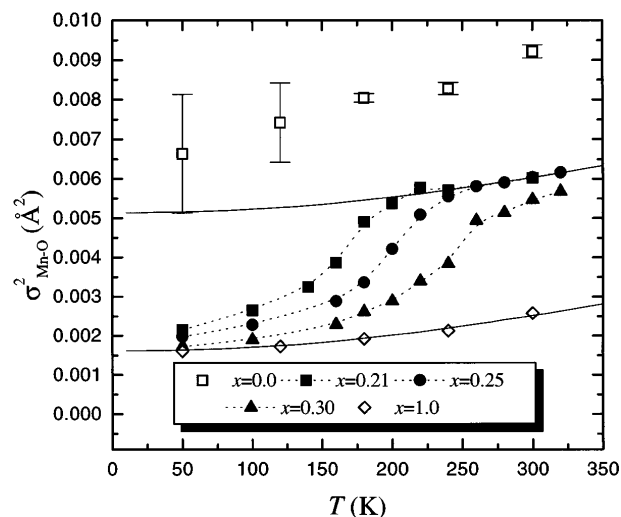
temperature for each sample, although occasionally only two were collected. Absorption from other excitations (pre-edge absorption) was removed by fitting the data to a Victoreen formula, and a simple spline was used to simulate the embedded-atom absorption μ_0. The XAFS oscillations χ were then obtained as a function of photoelectron wave vector $k = \sqrt{2m_e(E - E_0)/\hbar^2}$ from $\chi(k) = \mu/\mu_0 - 1$. The $k\chi(k)$ data were Fourier transformed (FT) (r space), and fit to suitably transformed standard functions calculated using the FEFF6 code [15]. All fits use an $S_0^2 = 0.72$, obtained from fits to the $CaMnO_3$ data, assuming six Mn-O bonds of equal length. S_0^2 accounts for scattering processes other than a single photoelectron excitation, and sets the overall scale for measurements of the bond length distribution widths described below. Further details of the methods used to reduce and fit the data can be found in Ref. [16].

Figure 1(b) shows the Fourier transform (FT) of $k\chi(k)$ vs r for the $La_{0.75}Ca_{0.25}MnO_3$ sample. In XAFS measurements, the peaks in the amplitude of the FT are phase shifted to lower r due to scattering of the photoelectron

FIG. 2. σ^2 vs T for the Mn-O bond length distribution. Solid lines show a fit to a correlated-Debye model ($\Theta_D = 940$ K) for $CaMnO_3$. This fit is shifted upwards to show that above T_c, the CMR samples have a similar temperature dependence. Dotted lines are guides to the eye. Relative errors are estimated to be smaller than the symbols, except for $LaMnO_3$.

we will explore in a future paper [19]. Below, we present a relation between the polaron distortion and M that better illustrates the possible physics.

Figure 3(a) shows the amplitude of the Mn-O peak of the FT at $T = 300$ K versus the calcium concentration x. The amplitudes are described well by a linear interpolation of the amplitudes of the end members. This linear relationship is consistent with a model whereby a JT distortion occurs around each Mn^{3+} ion in the doped materials, but not around each Mn^{4+} ion. Of course, intermediate distortions around each ion are also possible. In any case, the amplitude of the Mn-O peak is an accurate predictor of the localized hole concentration. Also shown in Fig. 3 is a line describing the amplitude of the Mn-O FT peak if the JT distortion was completely removed due to delocalization of the charge carriers. An increased bond length causes a reduction of the FT amplitude, because the XAFS amplitude is proportional to $1/r^2$. In this situation, all Mn-O bond lengths would be equal, and given by a linear interpolation between 1.97 Å (from $LaMnO_3$ lattice constants) and 1.89 Å (from $CaMnO_3$).

Below T_c, the three CMR samples have a much higher amplitude ($\sim 40\%$) due to partial removal of the JT

distortions in the octahedra. Meanwhile, the amplitudes of the other samples still can be described by a linear interpolation of the amplitudes of the end members, with the same slope.

Now we use these amplitudes to calculate the number of delocalized holes (n_{dh}) in the metallic state that evolve from trapped holes. As a trapped hole becomes delocalized, it will no longer contribute to the Mn-O distortion. If all available holes become conducting, we hypothesize that the amplitude of the peak would be given by the dashed line in Fig. 3(a). We will call this amplitude $A_{ND}(x, T)$ (not distorted), while the full distortion described by the dotted line is defined as $A_D(x, T)$. The actual amplitude at any given temperature is defined as $A(x, T, M)$, where the magnetization dependence causes the polaron distortions to be removed. We estimate the number of delocalized holes n_{dh} per Mn site to be given by

$$n_{dh} = \frac{A(x, T, M) - A_D(x, T)}{A_{ND}(x, T) - A_D(x, T)} x, \qquad (1)$$

where x (calcium concentration) gives the maximum number of available holes per Mn site. Since the amplitude of the Mn-O peak is proportional to $1/\sigma$, we can rewrite Eq. (1) using the fit results as

$$n_{dh} = \frac{1/\sigma - 1/\sigma_D}{1/\sigma_{ND} - 1/\sigma_D} x. \qquad (2)$$

The widths σ_D and σ_{ND} can be written in terms of the thermal contribution σ_T, and the fully developed polaron contribution σ_{FP}:

$$\sigma_D^2 = \sigma_T^2 + \sigma_{FP}^2,$$
$$\sigma_{ND}^2 = \sigma_T^2.$$

We model σ_T by using a fit to the $CaMnO_3$ data, and define $\sigma_{FP}^2 = \sigma^2 - \sigma_{CaMnO_3}^2$ at $T = 300$ K for each sample.

The key finding of this Letter is the linear relationship between $\ln(n_{dh})$ from Eq. (2)] and M [from Fig. 1(a)] shown in Fig. 3(b). In addition, the rate of change of $\ln(n_{dh})$ with M/M_0 is approximately the *same* for each of the samples. A careful examination of the figure will show that $\sim 20\%$ of the available holes are still localized at 50 K in this picture, decreasing slightly with increasing calcium concentration over this concentration range.

Since $\ln(\rho) \propto -M$ [8], these data suggest that $\rho \propto 1/n_{dh}$, as one might expect. This proportionality of course also implies that ρ is directly related to the polaron distortion via Eq. (2).

We must point out that the XAFS measurements were performed in *zero* applied field, while the magnetization curves [and the $\ln(\rho) \propto -M$ relation] were obtained under an applied field. However, muon-spin relaxation experiments [20] have confirmed the ρ relation with no applied field, by using the muon precession frequency as a relative measure of the magnetization.
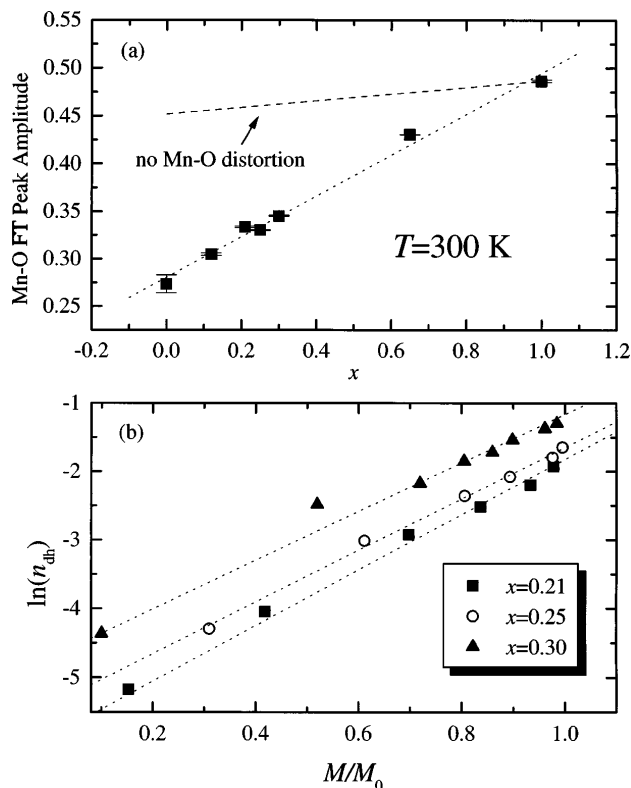
FIG. 3. (a) Amplitude of Mn-O FT peak at $T = 300$ K vs x. Dotted line is a linear fit, showing that the amplitude is described well by linearly interpolating the amplitudes of the end members. The dashed line shows the approximate amplitude expected if all distortions were removed. (b) $\ln(n_{dh})$ vs normalized magnetization M/M_0, where n_{dh} is the number of delocalized holes per Mn site. See text for definition of n_{dh}.

The linear relationship in Fig. 3(b) and the agreement with a similar relationship between ρ and M [8] support the simple model used [Eq. (1)]. This model assumes each delocalized hole removes the JT distortion on a single Mn^{3+} site, or at least that the actual distortions are on average proportional to this model distortion. This model is functionally the same as used by Hundley et al., which explains $\ln(\rho) \propto -M$ in terms of a decreasing polaron binding energy W_p with increasing M [21]. If Hundley et al.'s model is correct, W_p is directly related to the distortion. Hundley et al.'s model is valid only when W_p is greater than the characteristic optical phonon energy, which is true only above ~ 150 K [21]. However, the functional relations $\ln(n_{dh}) \propto M$ and $\ln(\rho) \propto -M$ still hold below 150 K. In the model describing Eq. (1), "activated" polarons no longer carry a distortion with them. Hence, they may flow via collective transport. This transport mechanism is very different than polaron-hopping transport, and may therefore explain the continued linear dependences below $T \sim 150$ K.

Other transport models may be in agreement with these relationships. One other possible model of the transport is that the localized charges become partially delocalized in the metallic state, and that the distortions are reduced proportionally to the number of Mn sites that a charge strongly overlaps. Although we can construct a simple model describing the mean number of Mn sites that a hole overlaps [similar to Eq. (1)], it is not clear how such a model should a priori relate to ρ or M.

Of course, a more rigorous description describing the residual width of the Mn-O bond length distribution above that of $CaMnO_3$ within a DE model with a significant lattice coupling [7] should provide the best description. Calculating the magnitude of such a distortion within these models as a function of M has not been reported, as far as we know.

In conclusion, we have reported XAFS data which directly relate the changes in the distortions of the MnO_6 octahedra to the magnetization. The linear relationship between the Mn-O peak amplitude and the calcium concentration in the paramagnetic state indicates that this amplitude is a measure of the localized hole concentration. By extending this model below T_c, we give an expression for the number of delocalized charge carriers n_{dh} in terms of the various measurable contributions to these distortions. This measurement of $\ln(n_{dh}) \propto M$ is in agreement with transport measurements which show $\ln(\rho) \propto -M$. Although other models may give a similar dependence of the Mn-O distortions to the magnetization, these empirical relationships between the charge, spin, and lattice degrees of freedom underscore the importance of including all these effects in any real theory of these systems. In particular, it should be possible to calculate the distortions as a function of magnetization with a theory which includes DE and polarons [22].

  *Permanent address: Los Alamos National Laboratory, MS K764, Los Alamos, NM 87545.

  †Permanent address: Physics Department, Florida Atlantic University, Boca Raton, FL 33431.

[1] G. H. Jonker and J. H. van Santen, Physica (Utrecht) **16**, 337 (1950); P. Schiffer, A. Ramirez, W. Bao, and S.-W. Cheong, Phys. Rev. Lett. **75**, 3336 (1995).

[2] J. Volger, Physica (Utrecht) **20**, 49 (1954).

[3] C. Zener, Phys. Rev. **82**, 403 (1951); P. W. Anderson and H. Hasegawa, Phys. Rev. **100**, 675 (1955); P. G. de Gennes, Phys. Rev. **118**, 141 (1960).

[4] S. Jin et al., Science **264**, 413 (1994).

[5] R. M. Kusters et al., Physica (Amsterdam) **155B**, 362 (1989); K. Chahara et al., Appl. Phys. Lett. **63**, 1990 (1993); R. von Helmolt et al., Phys. Rev. Lett. **71**, 2331 (1993).

[6] A. J. Millis, P. B. Littlewood, and B. I. Shraiman, Phys. Rev. Lett. **74**, 5144 (1995).

[7] A. J. Millis, R. Mueller, and B. I. Shraiman, Phys. Rev. B **54**, 5405 (1996), and references therein; H. Röder, J. Zhang, and A. R. Bishop, Phys. Rev. Lett. **76**, 1356 (1996).

[8] M. F. Hundley et al., Appl. Phys. Lett. **67**, 860 (1995).

[9] M. Jaime et al., Appl. Phys. Lett. **68**, 1576 (1996).

[10] G. Zhao, K. Conder, H. Keller, and K. A. Müller, Nature (London) **381**, 676 (1996).

[11] S. J. L. Billinge et al., Phys. Rev. Lett. **77**, 715 (1996).

[12] T. A. Tyson et al., Phys. Rev. B **53**, 13 985 (1996).

[13] C. H. Booth, F. Bridges, G. J. Snyder, and T. H. Geballe, Phys. Rev. B **54**, R15 606 (1996).

[14] D. Louca et al., Phys. Rev. B **56**, R8475 (1997).

[15] S. I. Zabinsky, A. Ankudinov, J. J. Rehr, and R. C. Albers, Phys. Rev. B **52**, 2995 (1995).

[16] G. G. Li, F. Bridges, and C. H. Booth, Phys. Rev. B **52**, 6332 (1995).

[17] P. Norby, I. G. Krogh Andersen, E. Krogh Andersen, and N. H. Andersen, J. Solid State Chem. **119**, 191 (1995).

[18] K. R. Poeppelmeier, M. E. Leonowicz, J. C. Scanlon, and J. M. Longo, J. Solid State Chem. **45**, 71 (1982).

[19] C. H. Booth et al. (unpublished).

[20] R. H. Heffner et al., Phys. Rev. Lett. **77**, 1869 (1996).

[21] M. F. Hundley et al., Mater. Res. Soc. Symp. Proc. **474**, 167 (1997).

[22] A. J. Millis and H. Röder (private communication).